Analysis of Oil-Air Two-Phase Flow Characteristics inside a Ball Bearing with Under-Race Lubrication

Authors:

Heyun Bao, Xiaonan Hou, Fengxia Lu

Date Submitted: 2021-04-26

Keywords: ball spin, oil volume fraction, oil-air two-phase flow, under-race lubrication, ball bearing

Abstract:

Under-race lubrication can increase the amount of lubricating oil entering a bearing and greatly improve lubrication and cooling effects. The oil-air two-phase flow characteristics inside a ball bearing with under-race lubrication play a key role in lubrication and cooling performance. The motions of ball bearing subassemblies are complicated. Ball spin affects the oil volume fraction. In this paper, the coupled level set volume of fluid (CLSVOF) method is used to track the oil-air two-phase flow inside the ball bearing with under-race lubrication. The influence of various factors on the oil volume fraction inside the ball bearing with under-race lubrication is investigated, particularly rotating speeds, inlet velocity and the size of oil supply apertures under the inner ring. The influence of the ball spinning is analyzed separately. The result demonstrates that, on account of the centrifugal force, lubricating oil is located more on the outer ring raceway at rotational speeds of 5000 r/min, 10,000 r/min, 15,000 r/min and 20,000 r/min. The oil volume fraction inside the bearing gradually increases at an oil inlet velocity of 5 m/s, 10 m/s and 15 m/s. The circumferential distribution of oil is also similar. As the diameter of the oil supply aperture increases from 1.5 mm to 2 mm, the oil volume fraction increases inside the ball bearing. However, the oil volume fraction slightly decreases from 2 mm to 2.5 mm of oil supply aperture diameter. Ball spin does not affect the circumferential distribution trend of the lubricating oil, but slightly reduces the oil volume fraction. Furthermore, ball spin causes the surface fluid to rotate around its rotation axis and increases the speed.

Record Type: Published Article

Submitted To: LAPSE (Living Archive for Process Systems Engineering)

Citation (overall record, always the latest version):	LAPSE:2021.0215
Citation (this specific file, latest version):	LAPSE:2021.0215-1
Citation (this specific file, this version):	LAPSE:2021.0215-1v1

DOI of Published Version: https://doi.org/10.3390/pr8101223

License: Creative Commons Attribution 4.0 International (CC BY 4.0)

processes

MDPI

Article

Analysis of Oil-Air Two-Phase Flow Characteristics inside a Ball Bearing with Under-Race Lubrication

Heyun Bao *, Xiaonan Hou and Fengxia Lu

National Key Laboratory of Science and Technology on Helicopter Transmission, Nanjing University of Aeronautics and Astronautics, Nanjing 210016, China; houxn2018@nuaa.edu.cn (X.H.); meefxlu@nuaa.edu.cn (F.L.)

* Correspondence: baoheyun@nuaa.edu.cn; Tel.: +86-138-5180-5472

Received: 17 August 2020; Accepted: 27 September 2020; Published: 1 October 2020

Abstract: Under-race lubrication can increase the amount of lubricating oil entering a bearing and greatly improve lubrication and cooling effects. The oil-air two-phase flow characteristics inside a ball bearing with under-race lubrication play a key role in lubrication and cooling performance. The motions of ball bearing subassemblies are complicated. Ball spin affects the oil volume fraction. In this paper, the coupled level set volume of fluid (CLSVOF) method is used to track the oil-air two-phase flow inside the ball bearing with under-race lubrication. The influence of various factors on the oil volume fraction inside the ball bearing with under-race lubrication is investigated, particularly rotating speeds, inlet velocity and the size of oil supply apertures under the inner ring. The influence of the ball spinning is analyzed separately. The result demonstrates that, on account of the centrifugal force, lubricating oil is located more on the outer ring raceway at rotational speeds of 5000 r/min, 10,000 r/min, 15,000 r/min and 20,000 r/min. The oil volume fraction inside the bearing gradually increases at an oil inlet velocity of 5 m/s, 10 m/s and 15 m/s. The circumferential distribution of oil is also similar. As the diameter of the oil supply aperture increases from 1.5 mm to 2 mm, the oil volume fraction increases inside the ball bearing. However, the oil volume fraction slightly decreases from 2 mm to 2.5 mm of oil supply aperture diameter. Ball spin does not affect the circumferential distribution trend of the lubricating oil, but slightly reduces the oil volume fraction. Furthermore, ball spin causes the surface fluid to rotate around its rotation axis and increases the speed.

Keywords: ball bearing; under-race lubrication; oil-air two-phase flow; oil volume fraction; ball spin

1. Introduction

In general, high-speed ball bearings are used in aeroengines as a significant component. Most of them are used with under-race lubrication [1]. One study [2] presented that the bearing has over 40% in the total heat-to-oil break down of a turbine engine. The bearing with the severe operating environment needs a host of oil to lubricate and reduce the temperature [3]. The under-race lubrication can improve the flow of lubricating oil in the bearing, such that the inner ring can be fully cooled and lubricated. For the high-speed ball bearing with under-race lubrication, the lubrication medium shows the characteristic of oil-air two-phase flow inside the bearing. The flow and heat characteristics of the two-phase flow inside the bearing are of significance for cooling and heat dissipation [4].

For angular contact ball bearing components, the motions are quite complex. The outer ring is static, and the inner ring, cage and balls rotate around the axis at their own speeds. In addition, the balls suffer from the spinning effect [5]. The internal channel of the bearing (called the bearing cavity in this paper) refers to the annular narrow channel between the inner and outer rings, that includes the fluid, ball and cage. Due to the complicated motion of the bearing, the oil-air two-phase flow in the bearing cavity is also complicated. Hu and Wu et al. [6,7] investigated the oil-air two-phase

flow inside an angular contact ball bearing with oil-jet lubrication by the VOF multiphase model. The investigations were based on the numerical method and temperature experiment. The results suggested that the oil-air distribution inside the angular contact ball bearing with oil-jet lubrication is not uniform. The oil volume fraction is lower, the temperature is higher. Yan et al. [5] established 1/18 periodic model of an angular contact ball bearing, and investigated the inside fluid flow and pressure distribution. Based on this, the lubrication device was optimized, and the limiting rotational speed of the angular contact ball bearing was increased by 6.0×10^3 r/min. Furthermore, Yan et al. [8] set up a high accurate numerical model using computation fluid dynamics (CFD) for different nozzle distributions and discussed temperature distribution, air-flow characteristics and oil volume fraction with the sealing condition. The result indicated that the lubricant oil can easily access the contact region between balls and rings, on account of a seal structure inside the bearing cavity. Adeniyi et al. investigated oil droplet motion inside the bearing [2], and oil-air flow between the cage and inner ring of an aero-engine bearing [9], by the CLSVOF method. Gao et al. [10] investigated oil distribution inside a roller bearing with under-race lubrication and discussed the effects of rotational speeds, oil inlet velocity and viscosity by a numerical method. Furthermore, NASA carried out some experimental studies on contact angular ball bearings. Parker [11] derived an equation for the lubricant percent volume in the bearing cavity XCAV, which is a function of lubricant flow rate, shaft speed and bearing pitch diameter. Pinel et al. [12] analyzed 35-mm-bore, angular-contact ball bearing lubricated by lubrication or through the split inner ring. For the bearing with under-race lubrication, the equation of XCAV was improved by considering more parameters [13].

At present, the research on the oil-air two-phase flow in the bearings cavity mostly focuses on oil injection lubrication, including the study of the lubrication structure and oil injection parameters. For the under-race lubrication, the motion of oil droplets inside the ball bearing and the oil-air two-phase flow has also been studied. For the high-speed ball bearing with under-race lubrication, the lubricant medium becomes oil-air two phase flow because of the complex motion including ball spin. As a result of this, the oil volume fraction and distribution inside the bearing directly affects the lubrication characteristics, while bearing speed and parameters of under-race lubrication affect the oil volume fraction and distribution. Furthermore, ball spin will have an influence on fluid motion on the ball surface, which is also one of the factors that cannot be ignored. In current works, for the bearing with under-race lubrication, there are few studies of the oil volume fraction and distribution about oil-air two phase flow. Based on this, this paper uses a numerical method to perform further research on the oil-air two-phase flow characteristics of the high-speed ball bearing with under-race lubrication, and discusses the effects of bearing rotational speed, oil inlet velocity, aperture diameters on oil distribution and volume fraction. Furthermore, this paper calculates the coordinates and rotation axis of the ball spin, through mathematical methods such as sine theorem and coordinate calculation, and then studies the influence of ball spin on oil distribution and volume fraction.

2. Numerical Model

For bearings with under-race lubrication, lubricant oil flows into the bearing cavity through the apertures of inner ring due to centrifugal force and high pressure. The apertures are perpendicular to the inner raceway surface and rotate along with the inner rings [10]. Based on references [14] and [2], a 3D numerical model of the ball bearing with under-race lubrication is established. As seen in Figure 1, the bearing consists of 18 balls, two rings as inner and outer rings, and a cage. There is a gap between the balls and the inner race, and two apertures are evenly distributed on the inner ring. Table 1 enlists the main parameters of the bearing. The fluid domain contains the flow field between the inner and outer raceways and hollows all the balls and cage. The fluid in the oil supply apertures under the ring is similar to a nozzle, as shown in Figure 2. Lubricant oil is supplied through the nozzles into the contacts between the balls, the inner and outer races and the cage. The Hertzian theory [15] describes the deformation of geometries in contact mechanics for elastic materials. Relevant research [16] indicated that the surface waviness values of the metallic bearing race are less than 2 μm.

Elastic deformations due to the contact of the balls and the raceways can be negligible, considering the order of magnitude of the deformations relative to the fluid domain volume size of the ball bearing [2].

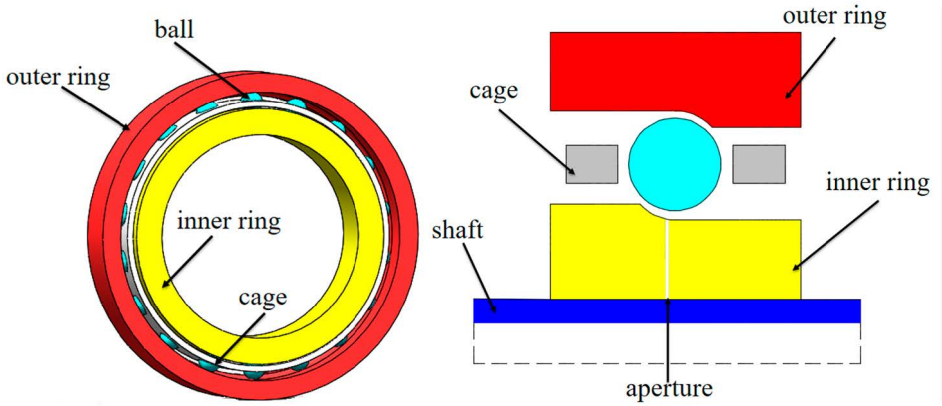

Figure 1. Configuration of ball bearing with under-race lubrication.

Table 1. Geometry parameters of ball bearing.

Geometry Parameters	Specification
Inner diameter/mm	140
Outer diameter/mm	225
Ball diameter/mm	15.4
Initial contact angle	26°
Ball number	18
Inner/outer race curve coefficient	0.515/0.525

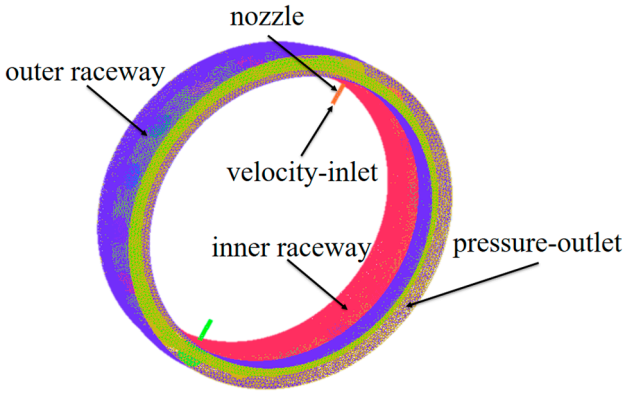

Figure 2. Computational mesh structure.

3. Numerical Method

3.1. Meshing and Boundary Conditions

The mesh is built with ANSYS-Mesh. The fluid domain of the bearing cavity is discretized with unstructured tetrahedral mesh in consideration of its complicated structure, and the fluid in the inner race apertures is discretized with structured hexahedral mesh, and the mesh is refined in the contact regions between balls and races. The mesh density depends on the bearing construction. The total number of combination elements is about 1.15 million, with about 0.24 million nodes, and the convergence is worse with the small number of mesh, as shown in Figure 2. The boundary condition is shown in Table 2.

Table 2. Boundary condition.

Name	Boundary Condition
Ball	No-slip, moving wall
Cage	No-slip, moving wall
Inner race	No-slip, moving wall
Outer race	No-slip, stationary wall
Oil inlets	Velocity inlet

The oil inlet via the apertures is set as the velocity-inlet. The velocity value is determined by different operations. The oil volume fraction is set as 1 in the oil inlet. Both end faces of the fluid inside the bearing are specified as pressure-outlet. The bearing cavity is supposed to be directly open to ambient air [10], and the pressure of both pressure-outlets is standard atmospheric pressure. Sliding mesh is used to reflect the rotational motion of the fluid domain. In view of the different rotational speeds between the fluid in the ball bearing cavity and the apertures, the sliding mesh plane are used between them to complete data transfer. The standard wall function is applied for near-wall boundary, and a no-slip boundary condition is used at the wall. The walls of the inner ring, cage and ball are set as moving wall and no-slip. The rotational speed of the balls and cage [6] is given by

$$n_b = \frac{1}{2} n_i \left(1 - \frac{D_b cos\alpha}{d_m}\right) \quad (1)$$

where n_b (r/min) is the rotational speed of the balls and cage; n_i (r/min) is the rotational speed of the inner ring; D_b (mm) is the ball diameter; α (°) is the bearing contact angle; and d_m (mm) is the pitch diameter of the bearing.

The lubricant oil used is aero lubricant 4109 [14]. The oil density is 970 kg/m^3 and the viscosity is 0.033 Pa·s. The air is regarded as ideal, with a density of 1.225 kg/m^3.

3.2. Numerical Method

Aidarinis et al. [17,18] assumed that the oil behaves as a porous media, such that the flow can be modeled as a single-phase flow. However, this limits the capability to account for the dynamics of the oil inside the ball bearing [2]. The CLSVOF [19] method is used in this paper. In the VOF technique, a color function, α, based on the volume fraction of the fluid, is applied to describe the multiphase mixture of oil and air. The cell is empty when $\alpha = 0$; the cell is full with oil when $\alpha = 1$; and the cell contains an interface between oil and air when $0 < \alpha < 1$.

In the level set technique, a smooth signed function, φ, is applied to describe the fluid phases, where $\varphi > 0$ is the oil phase; $\varphi = 0$ is the free interface; and $\varphi < 0$ is the air phase.

The renormalization group (RNG) k-ε model is based on the instantaneous Navier–Stokes (N-S) equation using a mathematical "renormalization group" method, including the effect of swirl flow on turbulence [20]. The RNG k-ε model can improve the precision under rotational flow in consideration of the effects of high strain rate, large curvature overflow and other factors [21]. Furthermore, the RNG k-ε model is very appropriate for the VOF model [22]. Consequently, the RNG k-ε model is applied in this paper. The SIMPLEC (semi-implicit method for pressure linked equations-consistent) method is adopted for the coupling of pressure and velocity. The second-order upwind difference is adopted for the convection terms. Pressure is adopted for the PRESTO! (pressure staggering option) format. The mass flow conservation between the inlets and outlets was used as the calculation convergence condition. The convergence criterion for residual of each velocity component and the VOF function is set to be 10^{-5}, while the convergence criterion for the residual of the turbulent kinetic energy and the turbulent kinetic energy dissipation rate is set to be 10^{-4}. Based on the rotational speed of the bearing cavity [23], considering the convergence and stability, the time step size is set to be 10^{-6}. A total of 30 iterations per time step are used. The number of time steps is 60,000, that is, the simulation time is 0.06 s.

4. Results

The simulated working conditions in this paper, including speed, diameter of nozzles, and inlet velocity, are shown in Table 3.

Table 3. Simulated cases.

Rotational Speed (rpm)	Diameter of Nozzles (mm)	Inlet Velocity ($m \cdot s^{-1}$)
5000	2	10
10,000	1.5/2/2.5	5/10/20
15,000	2	10
20,000	2	10

4.1. Oil Distribution at Different Rotational Speeds

Figures 3 and 4 show the oil distribution and oil volume fraction trend inside the bearing with flow time, respectively. The operation was performed at 5000 r/min, 10 m/s of inlet velocity, and 2 mm of aperture, that is, about 1.9 L/min of oil supply. As shown in Figures 3 and 4, lubricant oil is distributed throughout the bearing within a short time. It gradually diffuses inside the bearing as the simulation time increases. Oil volume fraction increases with the increase in simulation time. Moreover, in Figure 3, the blue marks the lubricant oil. The more blue areas represent the more lubricant oil.

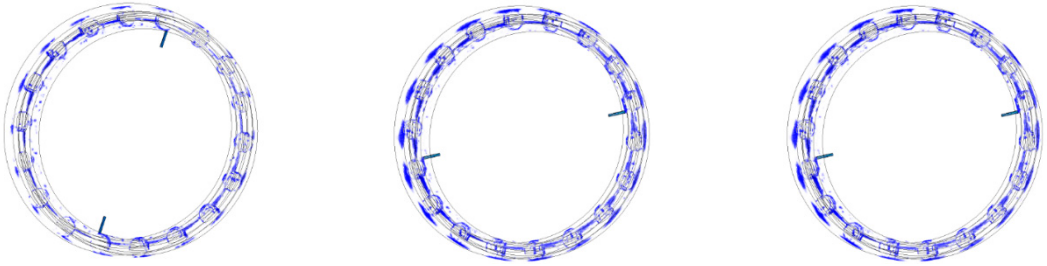

(**a**) 0.02 s (**b**) 0.04 s (**c**) 0.06 s

Figure 3. Oil distribution evolution inside the bearing with flow time.

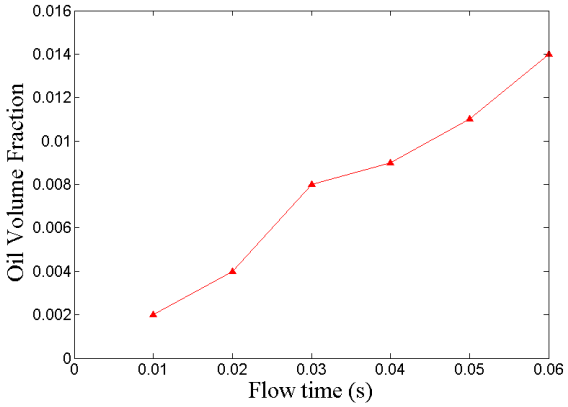

Figure 4. Oil volume fraction inside the bearing with flow time.

Figure 5 shows the oil distribution inside the bearing in the Y = 0 cross-section with different rotational speeds. Figure 6 shows the oil volume fraction around the circumference with different rotational speeds. The rotational speeds of the inner ring are 5000 r/min, 10,000 r/min, 15,000 r/min and 20,000 r/min. The inlet velocity is 10 m/s, and the diameter of the oil aperture is 2 mm, that is, the oil supply is about 1.9 L/min. The oil volume fraction inside the bearing is higher at 5000 r/min, but as

the speed of inner ring increases from 5000 r/min to 10,000 r/min, 15,000 r/min and 20,000 r/min, the oil volume fraction gradually decreases. At 20,000 r/min, the oil volume fraction inside the bearing sharply decreases, which is not conducive to lubrication and cooling. It can be seen from Figure 6 that the oil distribution becomes more uniform, and the curve fluctuation is smaller with the increase in speed. As can be seen in Figures 5 and 6, the oil volume fraction decreases as the rotation speed increases. According to the results of Adeniyi [2], lubricant oil exists in the form of irregular-shaped droplets inside the bearing. At lower speeds, the size of the oil droplets is more uniform, and the population is higher; that is, the oil volume fraction is higher. Therefore, the oil volume fraction is higher, and the lubrication is better. From Figure 5, lubricant oil inside the bearing is mainly concentrated on the outer ring raceway because of the centrifugal force, which will be conducive to the lubrication and cooling of the outer ring raceway and lowering the outer ring temperature, and will be further discussed in the ongoing study.

As the study of under-race lubrication with single aperture in Ref. [10], the lubricant oil is mainly concentrated on the outer ring raceway. At the speed of 5000 r/min, the oil volume fraction inside the bearing is higher than other speeds. It is consistent with the results of this paper.

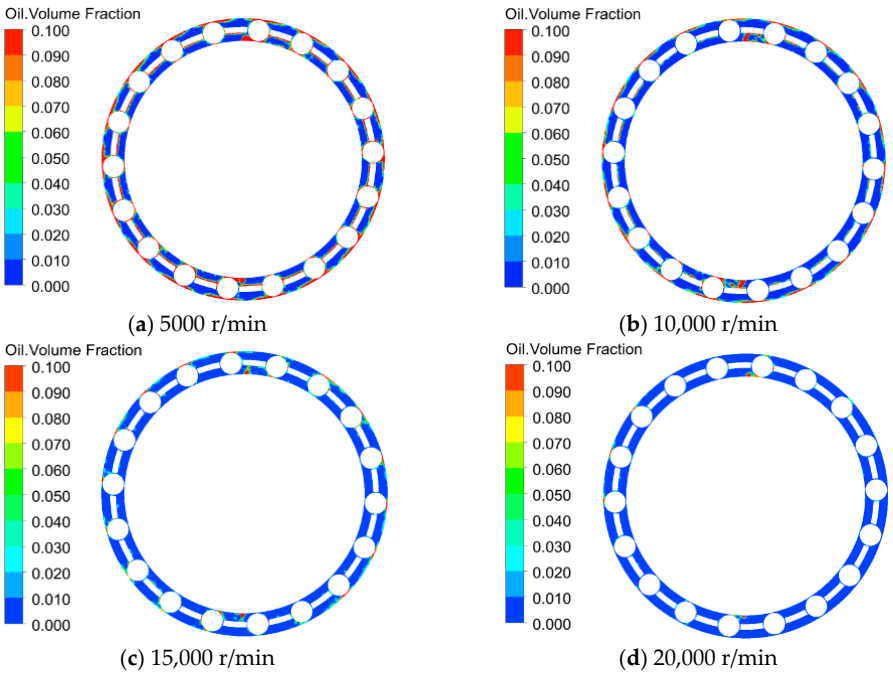

(**a**) 5000 r/min (**b**) 10,000 r/min

(**c**) 15,000 r/min (**d**) 20,000 r/min

Figure 5. Oil distribution in the Y = 0 cross-section with different rotational speeds.

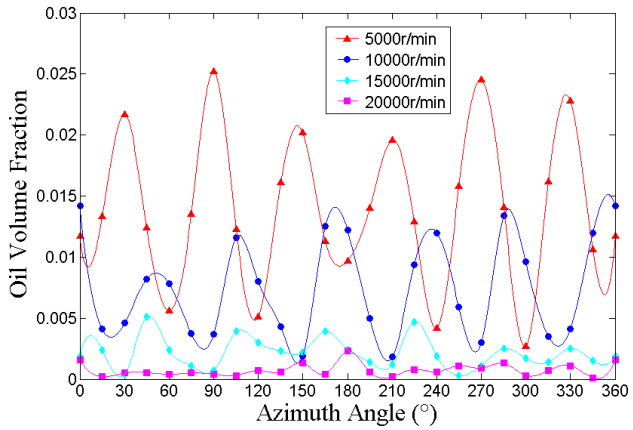

Figure 6. Oil volume fraction around the circumference with different rotational speeds.

4.2. Oil Inlet Velocity

Different oil inlet velocities will also affect the oil distribution and volume fraction inside the bearing. Consequently, the oil volume fraction is studied under the operating conditions of 10,000 r/min and the diameter of two apertures as 2 mm, with oil inlet velocity set at 5 m/s, 10 m/s and 15 m/s. Figure 7 shows the oil distribution inside the ball bearing with different oil inlet velocities, and the blue of Figure 7 is the same meaning as Figure 3. It shows that, as the inlet velocity increases, the oil volume fraction inside the bearing significantly increases. At 5 m/s, there is only a small amount of lubricant oil inside the bearing, which is not conducive to lubrication and heat dissipation. As shown in Figure 8, the oil distribution trend around the circumference inside the bearing is similar at the three inlet velocities. Then, the oil volume fraction increases with the increase in velocity. Furthermore, for the under-race lubrication, the oil supply should be more, to avoid insufficient lubrication.

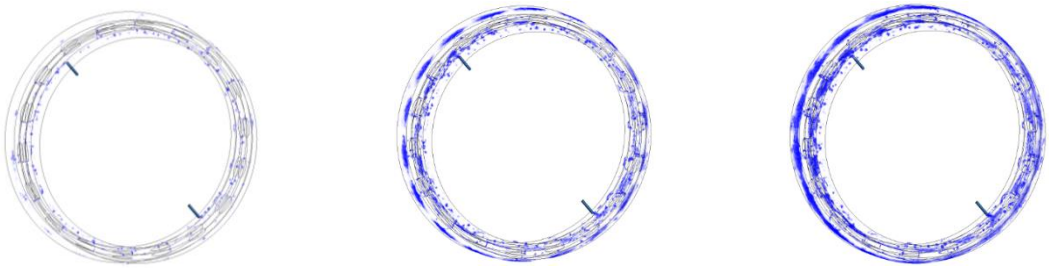

(a) 5 m/s (b) 10 m/s (c) 15 m/s

Figure 7. Oil distribution inside the ball bearing with different oil inlet velocities.

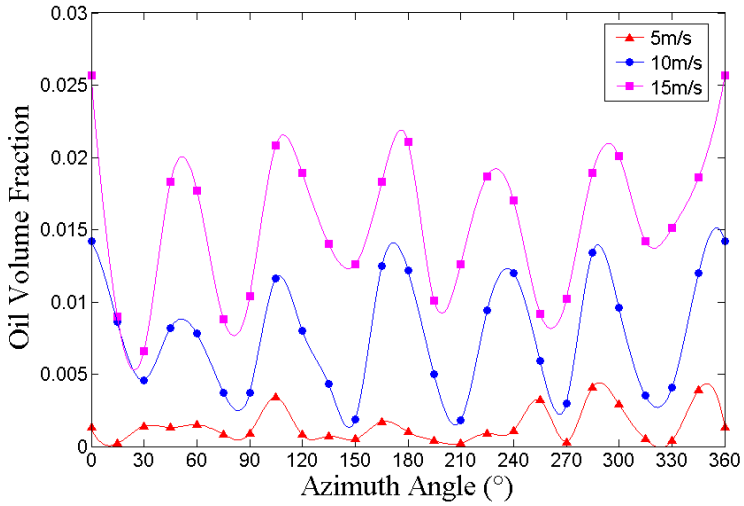

Figure 8. Oil volume fraction around the circumference with different oil inlet velocities.

4.3. Diameter of Apertures

When the rotational speed of the inner ring is 10,000 r/min and the oil inlet velocity is 10 m/s, the diameter of the oil inlet aperture under the ring will also have an effect on oil volume fraction inside the bearing. Figures 9 and 10 show the oil distribution and oil volume fraction around the circumference inside the bearing with different aperture diameters, respectively, and the blue of Figure 9 has the same meaning as Figure 3. It can be seen from the figure that, when the diameter of the oil inlet aperture is 2 mm, the oil volume fraction is the highest inside the bearing. When the diameter of aperture is 1.5 mm, there is only a small amount of lubricating oil inside the bearing, which is not conducive to lubrication and heat dissipation. As for the 2.5 mm diameter of aperture, the fluid-structure impact increases with the increase in diameter of aperture [10], which causes more lubricating oil to flow out of the bearing, and decreases the oil volume fraction. Combined with the analysis of the oil inlet

velocity, the combination of oil inlet velocity and the aperture diameter needs to be optimized to obtain the best lubrication and cooling performance for the bearing.

As for the studies of in Refs. [4,10], there is an optimal oil supply that makes the oil volume fraction highest. In this paper, the result shows that the 2.5 mm diameter of aperture and 10 m/s oil inlet velocity are not the optimal combination for the oil volume fraction. However, the combination of 2 mm and 10 m/s is better.

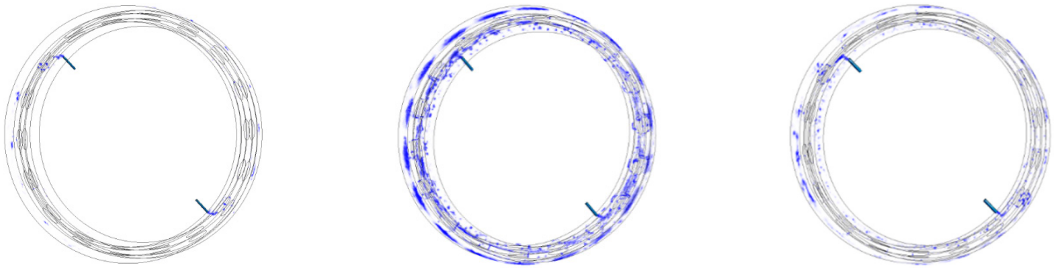

(**a**) 1.5 mm (**b**) 2 mm (**c**) 2.5 mm

Figure 9. Oil distribution inside ball bearing with different aperture diameters.

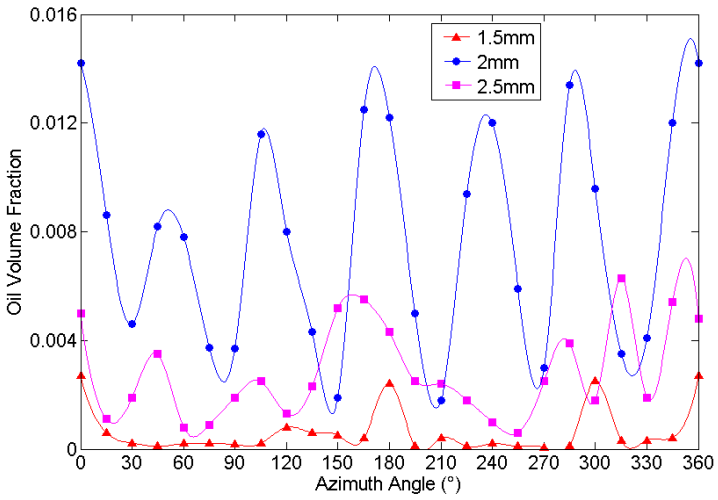

Figure 10. Oil volume fraction around the circumference with different aperture diameters.

4.4. Ball Spin

Under actual working conditions, due to the cage and the high-speed rotation of the inner ring, the ball not only has a revolution, but also has the spinning motion around a certain axis [2], as shown in Figure 11. According to [24], the angle between ball spin axis and the shaft axis $\beta = (\alpha_1 + \alpha_2)/2$. In this paper, the contact angle of the angular contact ball bearing is 26°. Simplify the bearing structure and take α_1, α_2 as 26°, then we can get $\beta = 26°$.

As shown in Figure 11, the origin of the ball spin is its geometric center. According to the sine theorem, the geometric center of the ball, *a*, is (−91.25·sin20°, 0, 91.25·cos20°) in the xOz rectangular coordinate system, and its spinning axis can be expressed as a vector (−sinβ·sin20°, −cosβ, sinβ·cos20°). Furthermore, the geometric center and axes of other balls can be obtained by symmetry. For the bearing with a stationary outer ring and a rotating inner ring, the speed of the ball spin can be determined by Equation (2) [25], where the negative sign indicates the opposite rotation direction of the inner ring:

$$n_w = -\frac{1}{2} n_i \left(\frac{d_m}{D_b} - \frac{D_b cos^2 \alpha}{d_m} \right) \quad (2)$$

When only considering the ball spin, the geometric center coordinates and rotation axes of the balls are applied as boundary conditions to the 18 balls. Figure 12 shows the oil volume fraction around the circumference inside the bearing, with or without ball spin. The distribution trend of oil volume fraction inside the bearing is generally consistent. When the ball spin is not considered, the oil volume fraction is slightly higher than when the spin is considered. As shown in Figure 13, when only considering the ball spin, the ball drives the fluid around its surface to rotate in the direction of its movement, which will agitate the fluid inside the bearing. As pointed out in the literature by Yan [5], in view of the motion of spinning, fluid around the ball flow velocity increases, and the flow direction is close to the spinning direction.

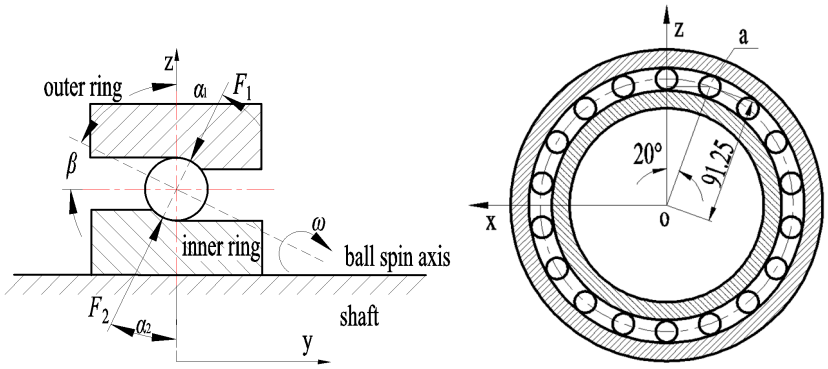

Figure 11. Schematic diagram of geometric parameters of the ball.

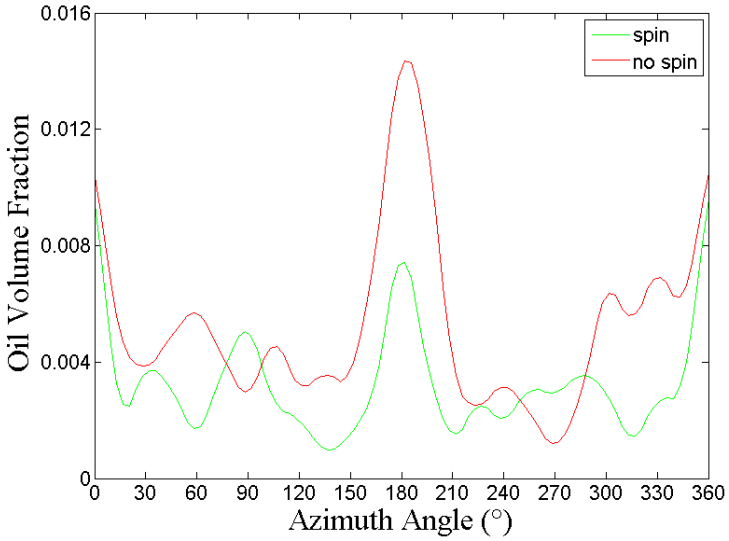

Figure 12. Oil volume fraction around the circumference, with or without spin.

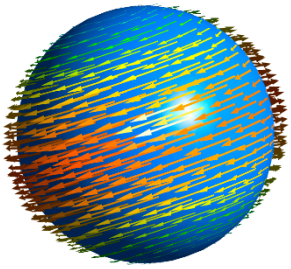

Figure 13. Surface streamline with ball spin.

5. Conclusions

For the ball bearing with under-race lubrication, the oil volume fraction and distribution inside the bearing will directly affect the lubrication characteristics, while complex bearing motion and parameters of under-race lubrication will affect the oil volume fraction and distribution. In this paper, the CFD method is applied to simulate the oil-air two-phase flow inside the ball bearing ring with under-race lubrication, and the CLSVOF method is used to track the two-phase flow. The sliding mesh is used to reflect the rotational motion of the fluid domain. The influence of rotating speeds, inlet velocity, size of oil supply apertures and ball spin on oil volume fraction is investigated. The following conclusions are drawn.

(1) Inside the bearing, the oil volume fraction is higher at 5000 r/min, but as the speed increases to 10,000 r/min, 15,000 r/min and 20,000 r/min, the oil volume fraction gradually decreases. Lubricant oil is mainly concentrated on the outer ring raceway because of the centrifugal force, which will be conducive to the lubrication and cooling of the outer ring.

(2) As the inlet velocity increases, the oil volume fraction inside the bearing increases. The trend of oil distribution around the circumference is similar at the three inlet velocities. As the diameter of the oil supply aperture increases from 1.5 mm to 2 mm, the oil volume fraction increases, but from 2 mm to 2.5 mm, the oil volume fraction slightly decreases. The oil inlet velocity and the diameter of the oil supply apertures should be reasonably selected to ensure a higher oil volume fraction.

(3) When the ball spin is not considered, the oil volume fraction is slightly higher than when the ball spin is considered. However, the oil distribution trend is generally consistent. In view of the spinning motion, fluid around the ball flow velocity increases, and the flow direction is close to the spinning direction.

Author Contributions: Writing-review & editing, H.B.; Writing-original draft, X.H.; Data curation, F.L. All authors have read and agreed to the published version of the manuscript.

Funding: This research was funded by National Natural Science Foundation of China (51975274).

Acknowledgments: This study was supported by the National Natural Science Foundation of China (51975274) and National Key Laboratory of Science and Technology on Helicopter Transmission (Nanjing University of Aeronautics and Astronautics) (Grant No. HTL-A-19K03).

Conflicts of Interest: The authors declare no conflict of interest.

References

1. Li, Y.J.; Chen, G.D.; Liu, Y.J.; Zhang, Y.H. Two-phase Fractional Flow Analysis of Aeroengine Main Bearing Inner-ring Oil-flow System. *Lubr. Eng.* **2009**, *34*, 58–61.
2. Adeniyi, A.A.; Morvan, H.P.; Simmons, K.A. A Multiphase Computational Study of Oil-Air Flow Within the Bearing Sector of Aeroengines. In Proceedings of the ASME Turbo Expo 2015: Turbine Technical Conference and Exposition, Montreal, QC, Canada, 15–19 June 2015.
3. Gloeckner, P.; Dullenkopf, K.; Flouros, M. Direct outer ring cooling of a high speed jet engine mainshaft ball bearing-experimental investigation results. In Proceedings of the ASME Turbo Expo 2010: Power for Land, Sea and Air, Glasgow, UK, 14–18 June 2010.
4. Wu, W.; Hu, C.H.; Hu, J.B.; Yuan, S.H.; Zhang, R. Jet cooling characteristics for ball bearings using the VOF multiphase model. *Int. J. Therm. Sci.* **2017**, *116*, 150–158. [CrossRef]
5. Yan, K.; Zhang, J.H.; Hong, J.; Wang, Y.T.; Zhu, Y.S. Structural optimization of lubrication device for high speed angular contact ball bearing based on internal fluid flow analysis. *Int. J. Heat Mass Transf.* **2016**, *95*, 540–550. [CrossRef]
6. Hu, J.B.; Wu, W.; Wu, M.X.; Yuan, S.H. Numerical investigation of the air–oil two-phase flow inside an oil-jet lubricated ball bearing. *Int. J. Heat Mass Transf.* **2014**, *68*, 85–93. [CrossRef]
7. Wu, W.; Hu, C.H.; Hu, J.B.; Yuan, S.H. Jet cooling for rolling bearings Flow visualization and temperature distribution. *Appl. Therm. Eng.* **2016**, *105*, 217–224. [CrossRef]
8. Yan, K.; Wang, Y.T.; Zhu, Y.S.; Hong, J. Investigation on the effect of sealing condition on the internal flow pattern of high-speed ball bearing. *Tribol. Int.* **2017**, *105*, 85–93. [CrossRef]

9. Adeniyi, A.A.; Morvan, H.P.; Simmons, K.A. A Computational Fluid Dynamics Simulation of Oil–Air Flow between the Cage and Inner Race of an Aero-engine Bearing. *J. Eng. Gas Turbine Power* **2017**, *139*, 1–8. [CrossRef]
10. Gao, W.J.; Nelias, D.; Li, K.; Liu, Z.X.; Lyu, Y.G. A multiphase computational study of oil distribution inside roller bearings with under-race lubrication. *Tribol. Int.* **2019**, *140*, 1–10. [CrossRef]
11. Parker, R.J. NASA Technical Paper. Available online: https://ntrs.nasa.gov/citations/19840010586 (accessed on 1 February 1984).
12. Pinel, S.I.; Signer, H.R.; Zaretsky, E.V. Design and Operating Characteristics of High-Speed, Small-Bore Ball Bearings. *Tribol. Trans.* **1998**, *41*, 423–434. [CrossRef]
13. Gao, W.J.; Lyu, Y.G.; Liu, Z.X.; Nelias, D. Validation and application of a numerical approach for the estimation of drag and churning losses in high speed roller bearings. *Appl. Therm. Eng.* **2019**, *153*, 390–397. [CrossRef]
14. Shi, X.J.; Wang, L.Q.; Mao, Y.Z.; Qin, F.Q. Coupling study on dynamics and TEHL behavior of high-speed and heavy-load angular contact ball bearing with spinning. *Tribol. Int.* **2015**, *88*, 76–84. [CrossRef]
15. Pandiyarajan, R.; Starvin, M.S.; Ganesh, K.C. Contact Stress Distribution of Large Diameter Ball Bearing Using Hertzian Elliptical Contact Theory. *Procedia Manuf.* **2012**, *38*, 264–269. [CrossRef]
16. Ren, Z.; Wang, J.; Guo, F.; Lubrecht, A.A. Experimental and Numerical Study of the Effect of Raceway Waviness on the Oil film in Thrust ball bearings. *Tribol. Int.* **2014**, *73*, 1–9. [CrossRef]
17. Aidarinis, J.; Goulas, A. Enhanced Computational Fluid Dynamics Modeling and Laser Doppler Anemometer Measurements for the Air-Flow in an Aero-engine Front Bearing Chamber—Part I. *J. Eng. Gas Turbine Power* **2015**, *137*, 1–14.
18. Aidarinis, J.; Goulas, A. Enhanced Computational Fluid Dynamics Modeling and Laser Doppler Anemometer Measurements for the Air-Flow in an Aero-engine Front Bearing Chamber—Part II. *J. Eng. Gas Turbine Power* **2015**, *137*, 1–15.
19. Sussman, M.; Puckett, E.G. A Coupled Level Set and Volume-of-Fluid Method for Computing 3D and Axisymmetric Incompressible Two-Phase Flows. *J. Comput. Phys.* **2000**, *167*, 301–337. [CrossRef]
20. Gong, Z.S. Study on Convective Heat Transfer Coefficient of High-Speed Train Wheels. Master's Thesis, Lanzhou Jiaotong University, Lanzhou, China, June 2017.
21. Xiao, J.L.; Zhu, E.Q.; Wang, G.D. Numerical simulation of emergency shutdown process of ring gate in hydraulic turbine runaway. *J. Fluids Eng.* **2012**, *134*, 1–9. [CrossRef]
22. Banerjee, R. A Numerical Study of Combined Heat and Mass Transfer in an Inclined Channel Using the VOF Multiphase Model. *Numer. Heat Transf. Part A* **2007**, *52*, 163–183. [CrossRef]
23. Guo, K.; Yuan, S.H.; Shao, Z.T. Study on Oil-Air Two-Phase Flow Inside the High-Speed Bearing Cavity with Jet Lubrication. *Trans. BIT* **2012**, *32*, 1022–1025.
24. Foord, C.A. High-speed ball bearing analysis. *J. Aerosp. Eng.* **2006**, *220*, 537–544. [CrossRef]
25. Tang, J. Lubrication analysis of oil-air two phase flow in high speed precision angular contact ball bearings. Master's Thesis, Jilin University, Jilin, China, May 2016.

© 2020 by the authors. Licensee MDPI, Basel, Switzerland. This article is an open access article distributed under the terms and conditions of the Creative Commons Attribution (CC BY) license (http://creativecommons.org/licenses/by/4.0/).